Poly(PEGA)-b-poly(L-Lysine)-b-poly(L-histidine) Hybrid Vesicles for Tumoral pH-triggered Intracellular Delivery of Doxorubicin Hydrochloride

ARTICLE *in* ACS APPLIED MATERIALS & INTERFACES · SEPTEMBER 2015

Impact Factor: 6.72 · DOI: 10.1021/acsami.5b05338

ACS APPLIED MATERIALS & INTERFACES

Research Article

www.acsami.org

Poly(PEGA)-*b*-poly(L-lysine)-*b*-poly(L-histidine) Hybrid Vesicles for Tumoral pH-Triggered Intracellular Delivery of Doxorubicin Hydrochloride

Renjith P. Johnson,[†,∥,⊥] Saji Uthaman,[§,⊥] Johnson V. John,[†] Hye Ri Lee,[†] Sang Joon Lee,[§] Huiju Park,[†] In-Kyu Park,[*,§] Hongsuk Suh,[‡] and Il Kim[*,†]

[†]BK 21 PLUS Center for Advanced Chemical Technology, Department of Polymer Science and Engineering, and [‡]Department of Chemistry and Chemistry Institute for Functional Materials, Pusan National University, Pusan 609-735, Republic of Korea

[§]Department of Biomedical Science and BK 21 PLUS Center for Creative Biomedical Scientists, Chonnam National University Medical School, 160 Baekseo-ro, Gwangju, 501-746, Republic of Korea

Supporting Information

ABSTRACT: A series of poly(ethylene glycol) methyl ether acrylate-*block*-poly(L-lysine)-*block*-poly(L-histidine) [p(PEGA)$_{30}$-*b*-p(Lys)$_{25}$-*b*-p(His)$_n$] (n = 25, 50, 75, 100) triblock copolypeptides were designed and synthesized for tumoral pH-responsive intracellular release of anticancer drug doxorubicin hydrochloride (Dox). The tumoral acidic pH-responsive hybrid vesicles fabricated were stable at physiological pH 7.4 and could gradually destabilize in acidic pH as a result of pH-induced swelling of the p(His) block. The blank vesicles were nontoxic over a wide concentration range (0.01−100 μg/mL) in normal cell lines. The tumor acidic pH responsiveness of these vesicles was exploited for intracellular delivery of Dox. Vesicles efficiently encapsulated Dox, and pH-induced destabilization resulted in the controlled and sustained release of Dox in CT26 murine cancer cells, and dose-dependent cytotoxicity. The tumor-specific controlled release Dox from vesicles demonstrates this system represents a promising theranostic agent for tumor-targeted delivery.

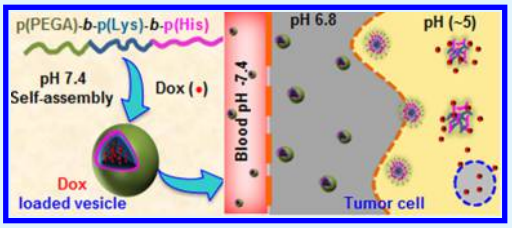

KEYWORDS: *biocompatible polymer, self-assembly, nanovesicles, pH-responsive, anticancer drug delivery*

1. INTRODUCTION

In the past few decades, a variety of tumor-targeting drug-delivery vehicles, such as liposomes[1] (vesicles formed from natural or synthetic lipids), polymeric micelles,[2−4] and, recently, polymersomes[5] (vesicles of completely synthetic amphiphilic (multiple) block copolymers), have been developed for the intracellular delivery of anticancer chemotherapeutics. Among these vehicles, intracellular pH-responsive nanovehicles made from biodegradable, synthetic polymers have attracted special interest, due to their promising pharmacokinetics and pharmacodynamics, arising from effective resistance to rapid renal clearance, along with nonspecific uptake by the reticuloendothelial system (RES), enabling these nanovehicles to passively target the tumor tissue by an enhanced permeation and retention (EPR) effect.[6] In recent years, liposomes,[1] micelles,[2−4] and polymersomes[5] have demonstrated different drug-delivery performance characteristics. Although liposomes and micelles have been investigated as a major platform for the delivery of anticancer drugs and imaging agents, it is recognized that pure liposomes suffer from very rapid blood clearance in vivo by the RES, unless a surface-modification approach is applied.[7−10]

To date, several amphiphilic block copolymers and their well-defined vesicles have been successfully synthesized.[11−14] For example, vesicles of poly(ethylene oxide)-*b*-polyethylethylene,[13] polystyrene-*b*-poly(ethylene oxide),[15] polystyrene-*b*-poly(acrylic acid), polystyrene-*b*-(4-vinylpyridine decyl iodide),[16] polybutadiene-*b*-poly(L-glutamate),[17,18] poly(acrylic acid)-*b*-polybutadiene,[19] polyisoprene-*b*-poly(L-lysine),[20] and polybutadiene-*b*-poly(L-lysine)[21,22] were fabricated through diverse self-assembly protocols. However, lack of fully biocompatible components or a desired stimulus-responsiveness was a major drawback, limiting the biomedical utility of these vesicles. Holowka et al. reported the formation of pH-responsive vesicles from block copolypeptides by conformation-specific assembly.[23] Subsequently, the synthesis of polypeptide-containing hybrid materials has evolved, with advances in novel synthetic tools[24−28] that can achieve well-defined hybrid architectures and are able to form "smart" nanocarriers. In recent years, several studies have reported the generation of pure polypeptidic or hybrid vesicles[29−38] for the intracellular anticancer delivery of doxorubicin hydrochloride (Dox).[31,32,35,36]

Biocompatible vesicles composed of PEG or its derivatives are ideal candidates for therapeutic delivery, due to their prolonged circulation time in vivo. The existence of pH gradients in biological systems,[39,40] and the presence of more-acidic environments in cancer cells as compared to healthy

Received: June 16, 2015
Accepted: September 16, 2015

DOI: 10.1021/acsami.5b05338
ACS Appl. Mater. Interfaces XXXX, XXX, XXX−XXX

Scheme 1. Synthetic Procedure for $p(PEGA)_{30}$-*b*-$p(Lys)_{25}$-*b*-$p(His)_n$, by the Click Cycloaddition Reaction of Alkyne-Terminated p(PEGA) and Azide-Terminated $p(Lys)_{25}$-*b*-$p(His)_n$

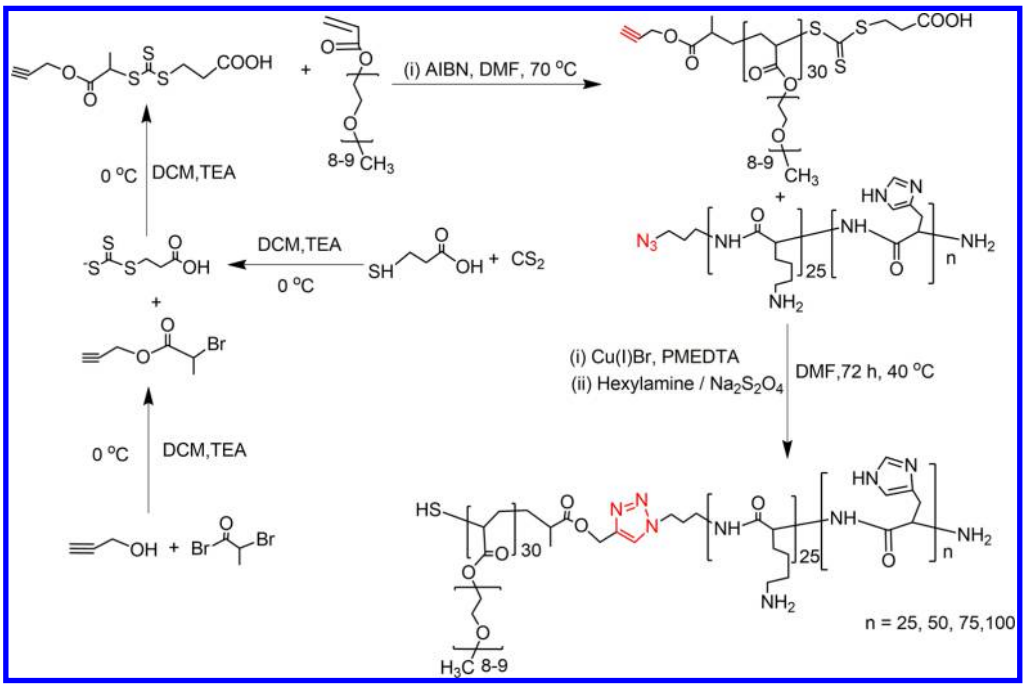

tissues, suggest that pH could be a useful stimulus for specific intracellular delivery of chemotherapeutic drugs. Additionally, a delivery vehicle with PEG surface functionality and a polypeptide that is responsive to endosomal pH could be a good supplement to the EPR effect for tumor extracellular targeting. Vesicles made from block copolymers consisting of PEG linked to polypropylene sulfide,[41] polycaprolactone,[42] polylactide,[42,43] polycarbonates,[44,45] polyaspartic acid,[46] PEO-*b*-poly(benzyl-L-glutamate)-*b*-(poly(L-lysine hydrochloride),[47] and poly(L-lysine)-*b*-poly(propylene oxide)-*b*-poly(L-lysine)[48] triblock copolypeptides have been reported, but none of these has shown the desired intracellular pH-responsiveness for efficient intracellular release. To the best of our knowledge, only a limited number of polymeric vesicles has been developed from pH-responsive polypeptide segments with a PEG surface functionality. Yin et al. fabricated vesicles from PEG-p(histidine) based AB_2-miktoarm polymers, which displayed successful pH-responsive in vitro release of encapsulated cargo.[49] Very recently, Quadir et al. reported endosomal pH-responsive PEG-*b*-polypeptide vesicles for pH-responsive intracellular release.[50]

Thus, development of new polymer vesicles with a rapid endocytosis and pH-responsive cellular internalization, along with good drug loading efficiency, has great interest for nanomedicine. In this study, we have developed biocompatible and tumoral acidic pH-responsive hybrid vesicle from a triblock terpolymer of ABC type, based on PEG methyl ether acrylate (p(PEGA)), poly(L-lysine)(p(Lys)), and poly(L-histidine)(p(His)) as A, B, and C blocks, respectively, ($p(PEGA)_{30}$-*b*-$p(Lys)_{25}$-*b*-$p(His)_n$ (n = 25, 50, 75, 100). Dox was encapsulated in the vesicles of $p(PEGA)_{30}$-*b*-$p(Lys)_{25}$-*b*-p(His), and the pH-responsive in vitro release was investigated. Cytotoxicity of the vesicles was tested with CT26 and NIH 3T3 cell lines, and the pH- and dose-dependent antitumor effect of released Dox has been assessed by CT26 cell lines.

2. EXPERIMENTAL SECTION

2.1. Materials. Propargyl alcohol (98.5%), 2-bromo propionyl bromide (98.5%), carbon disulfide (99.9%), 2-mercapto propionic acid (97%), triethylamine (TEA, 99.5%), 2,2′-azobis(2-methylpropionitrile) (AIBN, 98%), poly(ethylene glycol) methyl ether acrylate (PEGA, M_n = 454, ≥99%), 1-bromo-3-aminopropane hydrobromide, N^{ε}-(carbobenzoxy-L-lysine) (99.0%), hydrogen bromide (33 wt % in acetic acid), and trifluoroacetic acid (99%) were purchased from Sigma-Aldrich and used without further purification. Doxorubicin hydrochloride (Dox) was purchased from Lancrix chemicals. *N*-α-*t*-Butyloxycarbonyl-*N*-im-benzyl-L-histidine (Boc-L-His-(Bzl)-OH) was purchased from Bachem and used without further purification. Potassium hydroxide, sodium azide, magnesium sulfate, and triphosgene (>98%) were purchased from TCI (Tokyo, Japan). *N*,*N*-Dimethylformamide (DMF) was distilled over sodium. Tetrahydrofuran (THF), methanol, chloroform, and dichloromethane (DCM) were dried over calcium hydride and distilled under reduced pressure. 1,4-Dioxane was purified by distillation after removing the peroxide impurities by passing through a activated Al_2O_3 column. Deionized (DI) water (purified to a resistance of 18 MΩ (Milli-Q Reagent Water System, Millipore Corp., Billerica, MA)) was used in all necessary reactions, solution preparations, and polymer isolations.

2.2. Instrumentation and Measurements. Column chromatography was performed using a Combi-Flash Companion purification system (Teledyne ISCO). Fourier transform infrared (FT-IR) spectra were taken by using a Shimadzu IR prestige 21 spectrometer. ^{1}H and ^{13}C NMR spectra were recorded on a Varian INOVA 400 NMR spectrometer, and chemical shifts were reported in parts per million (ppm) relative to the residual solvent peaks as internal standard. ^{1}H NMR spectra peak multiplicities are denoted as br (broad), m (multiplet), t (triplet), d (doublet), and s (singlet). The molecular weight (MW) and polydispersity index ($Đ$) of the polymers were measured on a Waters GPC system, at 40 °C by using HPLC grade DMF containing 0.1 N LiBr as eluent. Monodispersed polystyrenes were used to generate the calibration curve. Dynamic light scattering (DLS) experiments were performed in a high performance Zetasizer Nano ZS90 (Malvern Instruments, Ltd., UK) with a He−Ne laser (633 nm) and 90° collecting optics and a thermoelectric pelteir temperature controller. Transmission electron microscopy (TEM) was

DOI: 10.1021/acsami.5b05338
ACS Appl. Mater. Interfaces XXXX, XXX, XXX−XXX

performed on a JEOL-1299EX TEM with an accelerating voltage of 80 keV.

2.3. Synthesis of p(PEGA)$_{30}$-*b*-p(Lys)$_{25}$-*b*-p(His)$_n$. The general synthetic procedure of p(PEGA)$_{30}$-*b*-p(Lys)$_{25}$-*b*-p(His)$_n$ triblock copolymer is shown in Scheme 1. Initially, for polymerizing PEGA by using the reversible addition−fragmentation transfer (RAFT) technique, a functional chain transfer agent (CTA), 2-propynyl-2-(2-caboxyethyl)dithiocaboxysulfanyl-propionate, was designed (see the Supporting Information for the detailed synthetic procedure).

2.4. Synthesis of Alkyne-Terminated p(PEGA) Using RAFT Polymerization. RAFT polymerization was conducted using standard Schlenk techniques. PEGA (4.54 g, 10 mmol), 2-propynyl-2-(2-caboxyethyl)dithiocaboxysulfanyl propionate (0.096 g, 0.33 mmol), and AIBN (5.5 mg, 0.03 mol) were loaded into a 25 mL Schlenk flask along with 5 mL of DMF as a solvent. The flask was sealed and subjected to three freeze−pump−thaw cycles. Polymerization was then started by immersion of the flask into a 70 °C oil bath. The polymerization was stopped by exposure to air and cooling to room temperature after 6 h. Polymer was isolated and purified by dialysis against methanol (Spectrapor, molecular weight cutoff (MWCO) = 6000 Da).

2.5. Synthesis of Azide-Terminated p(Lys)$_{25}$-*b*-p(His)$_n$ (*n* = 25, 50, 75, 100). For the ROP of Z-lys-*N*-carboxy anhydride (Z-Lys-NCA), 1-azido-3-aminopropane (25 μL, 0.25 mmol) and Z-Lys-NCA (1.91 g, 25 mmol) were dissolved in absolute DMF in two separate Schlenk flasks under nitrogen atmosphere. The solutions were then combined using a nitrogen purged transfer needle. After being stirred for 72 h at room temperature under nitrogen atmosphere, DMF was concentrated under high vacuum, and precipitated in diethyl ether. Isolated azide-terminated p(Z-Lys)$_{25}$-NH$_2$ was then vacuum-dried.

For the synthesis of p(Z-Lys)$_{25}$-*b*-p(Bn-His)$_n$ (*n* = 25, 50, 75, 100), azide-terminated p(Z-Lys)$_{25}$-NH$_2$ was used as a macroinitiator. p(Z-Lys)$_{25}$-NH$_2$ (0.36 g, 0.05 mmol) and a prescribed amount of Bn-His-NCA were dissolved in DMF in two separate Schlenk flasks and subsequently combined. After being stirred for 5 d at room temperature, the solvent was concentrated, and the polymer was precipitated in diethyl ether. Azide-terminated p(Z-Lys)$_{25}$-*b*-p(Bn-His)$_n$ (*n* = 25, 50, 75, 100) was isolated and vacuum-dried. For the deprotection of the protective side groups, a round-bottomed flask was charged with a solution of the azide-terminated p(Z-Lys)$_{25}$-*b*-p(Bn-His)$_n$ in trifluoroacetic acid (250 mg, 5 mL), and a 33 wt % solution of HBr in acetic acid (4-fold molar excess) was added and stirred for 16 h at room temperature. Finally, the reaction mixture was precipitated in diethyl ether, and the product was subsequently dialyzed against DI water and lyophilized to yield azide-terminated p(Lys)$_{25}$-*b*-poly(His)$_n$ (*n* = 25, 50, 75, 100) (see Schemes S1−S3).

2.6. Synthesis of p(PEGA)$_{30}$-*b*-p(Lys)$_{25}$-*b*-p(His)$_n$ (*n* = 25, 50, 75, 100). Click cyclo addition reactions between alkyne-terminated p(PEGA)$_{30}$ and azide-terminated p(Lys)$_{25}$-*b*-p(His)$_n$ were performed as follows. Alkyne-terminated p(PEGA)$_{30}$ (0.54 g, 0.04 mmol) and azide-terminated p(Lys)$_{25}$-*b*-p(His)$_{100}$ (0.84 g, 0.04 mmol) were solubilized in a 25 mL Schlenk flask containing dry DMF (15 mL) connected with a N_2 inlet and covered with a rubber septum. The mixture was stirred for 30 min, and PMDETA (10 μL, 0.08 mmol) was added through a sterile syringe under nitrogen environment. The mixture was degassed by three freeze−thaw cycles and added to another Schlenk containing CuBr (0.011 g, 0.08 mmol) via a nitrogen-purged syringe. The Schlenk flask was placed in an oil bath regulated at 40 °C for 3 d under static nitrogen pressure. After completion of the reaction, polymer solution was passed through a short silica column to remove copper catalyst. After concentration, the solution was poured into a diethyl ether and centrifuged. Finally, the product was then subjected to aminolysis in the presence of hexylamine and few drops of $Na_2S_2O_4$ in DMF. The reaction solution precipitated into diethyl ether, and the final polymer isolated was vacuum-dried and stored at −20 °C.

2.7. Fabrication of p(PEGA)$_{30}$-*b*-p(Lys)$_{25}$-*b*-p(His)$_n$ Vesicles. The vesicles of p(PEGA)-*b*-p(Lys)-*b*-p(His) were prepared by combining a self-assembly-derived nanoprecipitation with a membrane dialysis against doubly distilled water. For example, p(PEGA)$_{30}$-*b*-p(Lys)$_{25}$-*b*-p(His)$_{100}$ (1 mg) was dissolved in ethanol (1 mL), and phosphate-buffered saline (PBS) (0.5 mL, pH 7.4) was then added dropwise into the polymer solution under stirring. The mixture was then warmed to 50 °C for 2 h in static condition, and allowed to cool slowly. The turbid mixture was then dialyzed against DI water for 12 h using a dialysis membrane (Spectrapor, MWCO = 2000). The outer phase was replaced at 3 h intervals with fresh water. For TEM observation, one drop of the aqueous solution was deposited onto a Formvar carbon-coated copper grid. After 5 min, the excess solution was removed by touching a filter paper to the edge of the grid, and the sample was then observed directly after complete drying.

For the fabrication of Dox-loaded polymersomes, an ethanolic solution of p(PEGA)$_{30}$-*b*-p(Lys)$_{25}$-*b*-p(His)$_{100}$ (1 mg in 0.5 mL) and Dox solution (2 mg in 0.5 mL of ethanol) were combined, and stirred for 2 h in the dark. PBS (0.5 mL, pH 7.4) was then added under stirring and heated to 50 °C for 2 h in static condition and allowed to cool. The solution was then dialyzed by using a membrane (Spectrapor, MWCO = 2000) for 12 h to remove the free drug, and the Dox-loaded vesicles were subsequently lyophilized.

2.8. Determination of Drug Loading Content (DLC), Efficiency (DLE), and In Vitro Drug Release. For the quantification of the amount of drug encapsulated, aliquots of the drug-loaded vesicles were broken up by adding 1 mL of DMSO. The obtained solution was analyzed using UV−vis spectroscopy. The characteristic absorbance of Dox (485 nm) was recorded and compared to a standard curve generated in DMSO of varying drug concentrations. The percentages of DLC and DLE were calculated according to the following equations:

$$\text{DLC (\%)} = (\text{weight of Dox in the vesicles/weight of Dox-loaded polymersomes}) \times 100$$

$$\text{DLE (\%)} = (\text{weight of Dox in the vesicles/weight of Dox for drug-loaded polymersomes preparation}) \times 100$$

For in vitro drug release studies, Dox-loaded vesicles suspended in a dialysis tube were placed into PBS (20 mL) with the required pH value in a shaking bath operating at 70 rpm. The PBS was periodically replaced with a fresh solution, and the amount of released Dox was measured by UV−vis spectroscopy. The Dox concentration was determined according to the standard curves for the Dox solution at different pH values.

2.9. Cell Culture and Confocal Laser Scanning Microscopy (CLSM). NIH 3T3 fibroblast and CT26 colon cancer carcinoma cell lines were cultured in DMEM medium supplemented with 10% FBS at 37 °C and 5% CO_2 atmosphere. CT26 cells were seeded in a Lab-Tek Chamber Slide at a seeding density of 1×10^5 cells/well. After 24 h, Dox-loaded polymersomes were added to the CT26 cells and incubated in the dark for 4 h at 37 °C. The pH of the culture medium was adjusted with 0.1 M HCl or 0.1 M NaOH to a required pH prior to use. After incubation, the media was removed, and the cells were then washed three times with PBS followed by the treatment of 4% paraformaldehyde. The fluorescence was then visualized using a confocal laser scanning microscope.

2.10. Cell Viability Assay and Flow Cytometer Analysis. The cell viability profiles of the p(PEGA)$_{30}$-*b*-p(Lys)$_{25}$-*b*-p(His)$_n$ blank polymersomes and Dox-loaded p(PEGA)$_{30}$-*b*-p(Lys)$_{25}$-*b*-p(His)$_{100}$ polymersomes were assessed by MTS assay in both NIH3T3 fibroblast and CT26 colon cancer carcinoma cell lines. Both of the cells were maintained in DMEM medium supplemented with 10% FBS and seeded at a density of 5×10^3 cells/well in a 96-well plate for 12 h at 37 °C. For the cell viability assay, after the incubation, the media was replaced with 100 μL of blank polymersomes, and Dox-loaded polymersomes containing medium were incubated for 24 h at 37 °C. After incubation, 20 μL of MTS reagent was added to each well, and cell viability was measured by the absorbance at 490 nm using a 550 BioRad plate-reader. The cell viability in each well was calculated with respect to the control well value. The results were presented as the mean and standard deviation obtained from five different samples. For

DOI: 10.1021/acsami.5b05338
ACS Appl. Mater. Interfaces XXXX, XXX, XXX−XXX

flow cytometer analysis, Dox-loaded p(PEGA)$_{30}$-*b*-p(Lys)$_{25}$-*b*-p-(His)$_{100}$ vesicles treated CT26 cells were seeded at a density of 1 × 10^6 cells/well and incubated overnight. After incubation, the medium was removed, and the cells were washed with PBS three times. After the PBS wash, the cells were harvested and analyzed with a flow cytometer (FACScan). Dox fluorescence intensity was measured by using an excitation wavelength of 488 nm and an emission wavelength of 522 nm.

3. RESULTS AND DISCUSSION

3.1. Synthesis of Alkyne-Terminated p(PEGA) via RAFT Polymerization. From the synthetic viewpoint of self-assembling macromolecular amphiphiles, RAFT polymerization has emerged as one of the most promising techniques, due to the ease of experimental setup and applicability to a wide range of monomers.[25] Successful RAFT polymerization can be achieved only by using an appropriate CTA, either trithiocarbonate or a dithioester. Trithiocarbonate is versatile for the design of multiblock copolymers, directly or after appropriate end-group modifications. Recently, in this aspect, Boyer et al. reported the synthesis of a trithiocarbonate CTA bearing an azide and a dithiopyridine group at R and Z fragments, for the RAFT polymerization and subsequent bioconjugation.[51] In this study, we synthesized a trithiocarbonate RAFT CTA bearing an alkyne group on the R fragment. ^{1}H and ^{13}C NMR spectra of the RAFT CTA and their synthetic intermediates are provided in Figures S1−S3. From the ^{1}H NMR spectra, the final structure of the RAFT CTA showed the presence of protons characteristic of a carboxyl group at 10 ppm, and also protons corresponding to methylene groups. Furthermore, the presence of the alkyne moiety was confirmed in FT-IR spectra, which showed the alkyne stretching band at 3280 cm^{-1}. ^{13}C NMR analysis further confirmed the successful synthesis of the expected RAFT CTA. Our synthetic approach then began with polymerization of PEGA in the presence of the alkyne-terminated RAFT CTA, resulting in pPEGA with an alkyne group at the chain end (p(PEGA)-CTA; Scheme 1).

The RAFT polymerization of PEGA was conducted in dimethylformamide (DMF),[52] with [PEGA]:[CTA]:[AIBN] ratios of 30:1:0.1. After removing residual monomers and impurities by dialysis against methanol, the polymer was analyzed by ^{1}H NMR, and the number-average molecular weight (M_n) and the polydispersity were determined by gel-permeation chromatography (GPC). The molecular-weight distributions remained narrow (PDI = 1.28), demonstrating that RAFT polymerization of PEGA with the alkyne-terminated CTA results in well-defined p(PEGA). The M_n of p(PEGA)-CTA, calculated by ^{1}H NMR end-group analysis, was 18 400. The M_n value obtained by GPC was 16 700. The difference in M_n values was probably due to the comparison with inauthentic polymer standards.[52]

3.2. Synthesis of Azide-Terminated p(Lys)$_{25}$-*b*-p(His)$_n$ (*n* = 25, 50, 75, 100). The parallel synthesis of azide-terminated block copolypeptide p(Lys)$_{25}$-*b*-p(His)$_n$ was carried out using 1-azido-3-aminopropane as initiator (Scheme S1). Complete transformation of the hydrobromide and bromo groups of 1-bromo-3-aminopropane hydrobromide into amine and azide groups was confirmed by ^{1}H NMR and FT-IR spectral analyses (Figure S4). Initially, the ring-opening polymerization of Z-Lys-NCA was performed, and then azide-terminated p(Lys)$_{25}$-NH$_2$ was used as macroinitiator for the synthesis of p(Lys)$_{25}$-*b*-p(His)$_n$, with different p(His) chain lengths. All ring-opening polymerizations of the NCAs were performed in absolute DMF, proceeded in a controlled manner, and were completed in 3−5 days, depending on the degree of polymerization. Full conversion of the NCAs was monitored by disappearance of NCA-associated carbonyl peaks at 1795 and 1730 cm^{-1} on FT-IR. The polymers were purified by precipitation in ethyl ether twice, washed with hexane, and vacuum-dried. Polymers were characterized by ^{1}H NMR and FT-IR spectroscopy to confirm their structures and the presence of the terminal azide group. All polymerizations were completed under similar conditions, to yield p(Z-Lys)$_{25}$-*b*-p(Bn-His)$_n$, where n = 25, 50, 75, or 100. In the second step, the protective side-chains were removed by treating p(Z-Lys)$_{25}$-*b*-p(Bn-His)$_n$ with HBr/AcOH in trifluoroacetic acid, and the resultant block copolymer was characterized by ^{1}H NMR and FT-IR spectroscopy (Scheme S3 and Figure S5). After the deprotection of protective groups, the peak integral ratios of the methylene proton of p(Lys) (δ = 2.6 ppm, NH$_2$−CH$_2$) and histidine ring protons (δ = 6.90 ppm) were used to calculate M_n, which confirmed the expected molecular weight (see Table S1).

3.3. Synthesis of p(PEGA)$_{30}$-*b*-p(Lys)$_{25}$-*b*-p(His)$_n$ (*n* = 25, 50, 75, 100). Our aim was to base the polymer design on biocompatible components with polypeptide segments responsive to intracellular stimuli and a "stealthy" PEGA outer corona for long circulation time and enhanced EPR effects. As compared to linear PEG, p(PEGA) has benefits in vivo. The greater steric bulk of a multibranched PEG leads to better protection against enzymatic degradation and reduced immunogenicity. p(Lys) and p(His) were introduced as building blocks because of their low toxicity and immunogenicity, and their endosomal-pH-responsiveness.[39] Most importantly, p(His) should enable efficient membrane fusion,[53] induced by the "proton sponge" mechanism of the imidazole groups, helping the vesicles to escape from the cellular compartment membrane.[54] The positive charges carried by p(Lys) can also contribute to activation of the RES of the organism, promoting clearance of the vesicles from the blood compartment.[47]

The combination of RAFT and "click" cycloaddition reactions has become very popular in polymer synthesis as a tool for functionalizing synthetic macromolecules. The copper-(I)-catalyzed, 1,3-dipolar cycloaddition of azides and terminal alkynes is simple and efficient, enabling high-yield reactions, and an absence of side-reactions.[27,28] We utilized the combination of RAFT and click chemistry to capitalize on the flexibility of RAFT and the efficiency and specificity of click reactions, to synthesize p(PEGA)$_{30}$-*b*-p(Lys)$_{25}$-*b*-p(His)$_n$. The azide-terminated p(Lys)$_{25}$-*b*-p(His)$_n$ polymers were then subjected to click cycloaddition reactions with alkyne-terminated p(PEGA), yielding p(PEGA)$_{30}$-*b*-p(Lys)$_{25}$-*b*-p-(His)$_n$ (n = 25, 50, 75, 100), and these polymers were subjected to aminolysis to remove the thiocarbonylthio end groups, and purified by dialysis. Finally, the triblock copolypeptides were fully characterized by GPC, ^{1}H and ^{13}C NMR, and FT-IR spectroscopy. Notably, in the FT-IR spectra, the disappearance of the azide stretching band at 2100 cm^{-1} in p(PEGA)-*b*-p(Lys)-*b*-p(His) shows the completion of the azide−alkyne coupling (see Figures S6 and S7 for ^{1}H NMR and GPC characterizations). The composition and the polydispersity of the triblock copolymers are provided in Table 1.

In the design of p(PEGA)$_{30}$-*b*-p(Lys)$_{25}$-*b*-p(His)$_n$, the compositions of p(PEGA) and p(Lys) were kept constant,

DOI: 10.1021/acsami.5b05338
ACS Appl. Mater. Interfaces XXXX, XXX, XXX−XXX

Table 1. Molecular Characteristics of p(PEGA)$_{30}$-*b*-p(Lys)$_{25}$-*b*-(His)$_n$ (n = 25, 50, 75, 100) Block Copolymers Synthesized by Azide−Alkyne Click Cycloaddition Reaction

block copolymer	yield (%)	$M_n \times 10^{-4}$ (g/mol) theor.	GPC	PDI[a]
p(PEGA)$_{30}$-*b*-p(Lys)$_{25}$-*b*-(His)$_{25}$	62	2.03	3.07	1.20
p(PEGA)$_{30}$-*b*-p(Lys)$_{25}$-*b*-(His)$_{50}$	59	2.30	3.44	1.25
p(PEGA)$_{30}$-*b*-p(Lys)$_{25}$-*b*-(His)$_{75}$	63	2.65	3.80	1.31
p(PEGA)$_{30}$-*b*-p(Lys)$_{25}$-*b*-(His)$_{100}$	66	3.06	4.47	1.36

[a]Determined by SEC in DMF at 40 °C in the presence of 0.1 M LiBr.

while systematically increasing the degree of polymerization of p(His) from 25−100, to achieve the amphiphilicity required for self-assembly, effective cellular uptake, and endosomal-pH-responsiveness for release of the encapsulated Dox.

3.4. Fabrication of p(PEGA)$_{30}$-*b*-p(Lys)$_{25}$-*b*-p(His)$_n$ Vesicles. Herein, we have demonstrated the vesicle formation of hybrid triblock copolymers of ABC type, composed of dual hydrophilic blocks, with a hydrophobic p(His) block as the C segment. Few "dual-hydrophilic" triblock copolymer vesicles have been reported previously;[55] these methods differ from this design by having different hydrophilic segments on opposite sides of a hydrophobic domain, usually a nondegradable, or degradable polypeptide, block.[41,45,47] One exception is the recent work of Rodriguez et al. toward completely polypeptidic vesicles from ABC-block copolypeptide-bearing dual-hydrophilic segments.[56]

Among block copolymers synthesized, we utilized block copolymers with long p(His) chain length for in vitro drug release and for further cellular internalization studies. High solubility of polymers with short p(His) chain length prevented them from forming polymersomes by self-assembly[57] at the conditions employed in this study. As water is a common solvent for both p(PEGA) and p(Lys) blocks, whereas ethanol is a poor solvent for p(His), self-assembly occurred after the injection of aqueous buffer into the polymer solution, making use of the solubility difference between p(PEGA), p(Lys), and p(His) blocks. After the removal of ethanol by dialysis, the morphologies of the self-assembled constructs were characterized. The amount of aqueous buffer affects the microstructure of the vesicles. We concluded that 0.5 mL of aqueous buffer (for a polymer concentration of 1 mg/mL in ethanol) is ideal for the formation of vesicles. Similarly, Dox was encapsulated into p(PEGA)$_{30}$-*b*-p(Lys)$_{25}$-*b*-p(His)$_n$ (n = 75, 100) vesicles to investigate their drug-loading and in vitro drug-release performance. Dialysis against deionized water was performed to remove the unloaded drug and ethanol, and the Dox loading content and loading efficiency of the vesicles were determined (Table 2).

The dimensions of the blank and Dox-loaded vesicles were determined by dynamic light scattering (DLS) measurements. The DLS data showed that the blank polymersomes we obtained were between 200 and 300 nm in size. After the encapsulation of Dox, the vesicles were not significantly altered in size. However, decreasing the pH of the polymersome dispersion, for example, to pH 5.5, remarkably increased the size of the vesicles. We suggest that this is due to the repulsion between the charged imidazole groups of the p(His) bilayer, which leads to a high level of swelling of the vesicles in acidic media. We expected that the vesicles would have a microstructure with the more-hydrophilic PEGA oriented "outward" toward the water, a less-hydrophilic p(Lys) inner core, and the hydrophobic p(His) forming the bilayer structure. To clarify this, we performed the zeta potential measurement of the vesicle dispersion, which displayed very low surface charge values, confirming the presence of the p(PEGA) block in the outer periphery, and p(Lys) in the interior of the vesicles. If p(Lys) had been oriented to the outer periphery, the zeta potential would have a much higher value. The vesicular morphology of the p(PEGA)$_{30}$-*b*-p(Lys)$_{25}$-*b*-p(His) assemblies was further visualized by TEM. As shown in Figure 1, spherical vesicles of around 200 nm were clearly observed, which was consistent with the size analysis by DLS, as shown in the insets of Figure 1(a and c).

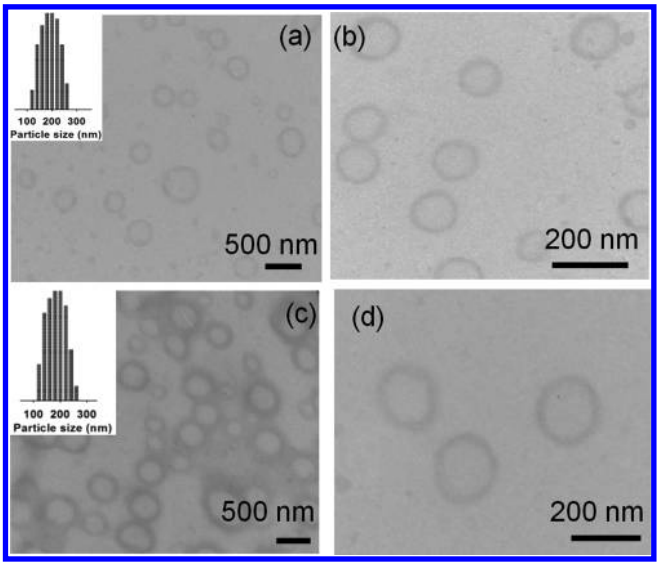

Figure 1. TEM images of the spherical vesicles of p(PEGA)-*b*-p(Lys)-*b*-p(His) triblock copolymers obtained by self-assembly in an ethanol/water solvent mixture at pH 7.4: (a,b) p(PEGA)$_{30}$-*b*-p(Lys)$_{25}$-*b*-p(His)$_{75}$, (c,d) p(PEGA)$_{30}$-*b*-p(Lys)$_{25}$-*b*-p(His)$_{100}$.

Table 2. Characteristics of the Blank and Dox-Loaded Vesicles of p(PEGA)-*b*-p(Lys)-*b*-(His) at Different pH Values

block copolymer	pH	blank vesicles R_H (nm)	PDI	Dox-loaded vesicles at 25:1 (w/w)[a] R_H (nm)	PDI	zeta potential (mV)	Dox loading content (%)	Dox loading efficiency (%)
p(PEGA)$_{30}$-*b*-p(Lys)$_{25}$-*b*-(His)$_{75}$	7.4	220 ± 2.6	0.09	250 ± 1.6	0.10	−4.58	15 ± 2	52
	5.5	350 ± 3.2	0.13	420 ± 3.2	0.40	+1.66		
p(PEGA)$_{30}$-*b*-p(Lys)$_{25}$-*b*-(His)$_{100}$	7.4	245 ± 2.6	0.11	270 ± 2.6	0.14	−3.81	21 ± 2	68
	5.5	372 ± 1.8	0.46	480 ± 1.8	0.65	+1.88		

[a]Feed ratio of polymer to Dox. Dox loading experiments were performed at pH 7.4.

DOI: 10.1021/acsami.5b05338
ACS Appl. Mater. Interfaces XXXX, XXX, XXX−XXX

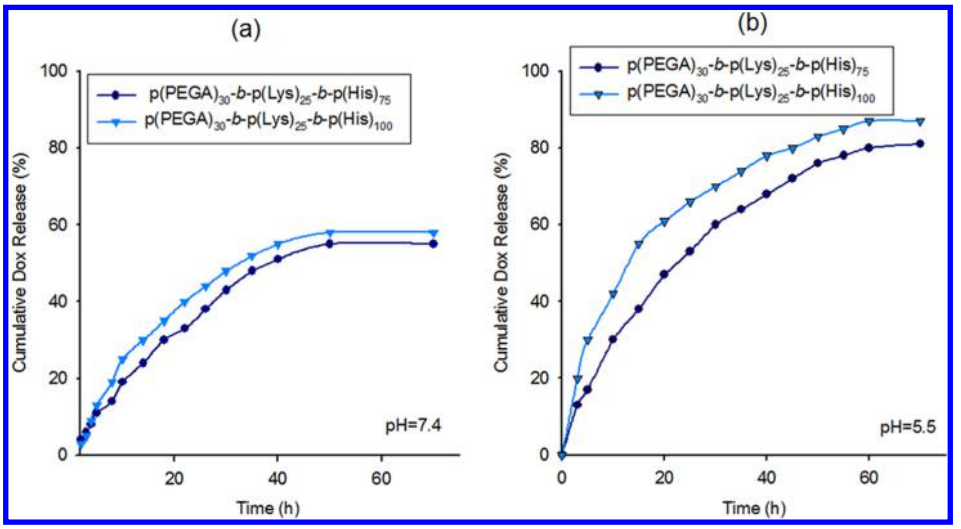

Figure 2. Time-dependent release of Dox from $p(PEGA)_{30}$-*b*-$p(Lys)_{25}$-*b*-$p(His)_{75}$ and $p(PEGA)_{30}$-*b*-$p(Lys)_{25}$-*b*-$p(His)_{100}$ vesicles in phosphate-buffered saline (PBS): (a) at pH 7.4 and (b) at pH 5.5, at 37 °C.

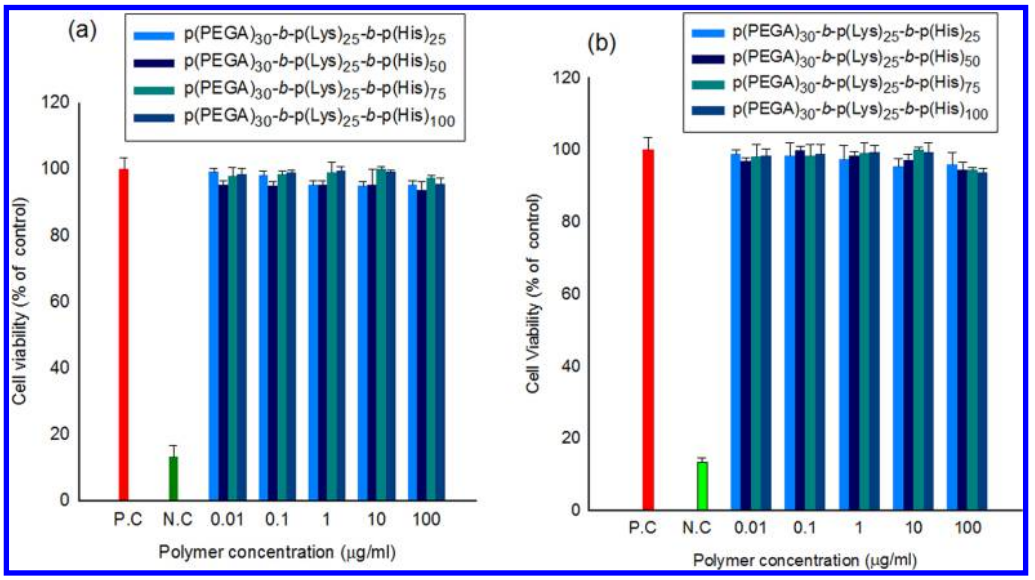

Figure 3. Cell viability, measured by the MTS assay of (a) NIH 3T3 and (b) CT26 cells exposed to $p(PEGA)_{30}$-*b*-$p(Lys)_{25}$-*b*-$p(His)_n$ at various concentrations. The cell-only group was used as the positive control (PC), and Triton X100 was used as the negative control (NC).

3.5. Dox Release Evaluation from $p(PEGA)_{30}$-*b*-$p(Lys)_{25}$-*b*-$p(His)_n$ Vesicles. To investigate the controlled Dox-releasing properties, Dox-loaded $p(PEGA)_{30}$-*b*-$p(Lys)_{25}$-*b*-$p(His)_n$ (n = 75, 100) vesicles were subjected to in vitro release studies in PBS at 37 °C. Release of Dox from the vesicles was observed over 70 h, and the release performance of Dox was traced using a UV−vis spectrometer at 485 nm, which is the characteristic absorption maximum of Dox in solution. The Dox-release profiles at two pH values are illustrated in Figure 2. At pH 7.4, around 30% of Dox remained in the vesicles after 72 h. At pH 5.5, the release rate was much faster; within the first 24 h, >50% of the initial load was released, reaching 80% within 72 h. These release profiles clearly indicate the desirable pH sensitivity for intracellular delivery, so that the vesicle is able to hold a substantial amount of encapsulated Dox over an extended period of time during systemic circulation (pH 7.4), whereas the rapid release of the drug can be triggered by tumoral acidic environment.

Note that the enhanced Dox release at pH 5.5 was triggered by the destabilization of the vesicle bilayers, as a result of the protonation of the p(His) moiety. Decreasing pH causes the imidazole ring of the p(His) block to be protonated, and the positively charged imidazole groups repel each other, leading to the pH-induced destabilization of the vesicle bilayer. Thus, at acidic pH, the degree of ionization of the p(His) block increases, and the vesicles lose the stability, which diminishes hydrophobic interactions, resulting in the rapid release of Dox. Moreover, the enhanced solubility of the p(PEGA) corona also helps to diffuse the Dox into the external medium. The size of p(His) block also affects Dox release rates to some degree. An increase in p(His) block increases diffusivity and therefore the drug release rate both at pH 5.5 and at pH 7.4. As the size of spherical vesicles increases with the increase of p(His) block, Dox diffusion through water-filled pores formed by vesicles destabilization, most probably more accelerated for bigger sized vesicles, increases accordingly. However, the size of p(His)

DOI: 10.1021/acsami.5b05338
ACS Appl. Mater. Interfaces XXXX, XXX, XXX−XXX

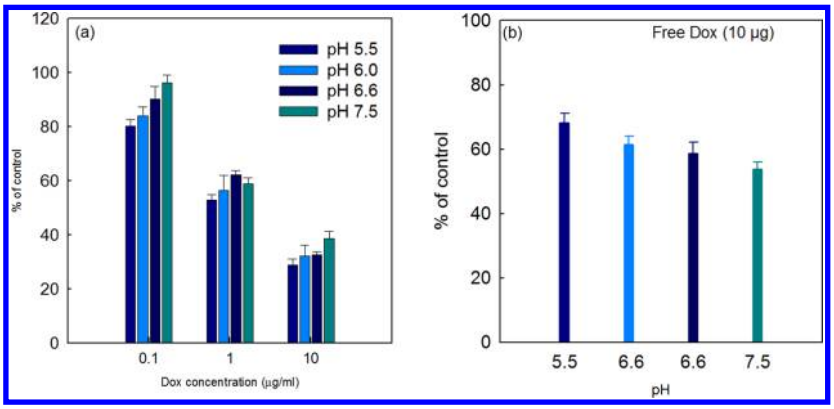

Figure 4. (a) Dose-dependent, pH-dependent antitumor activity of Dox-loaded vesicles to CT26 cells after 24 h incubation. (b) Antitumor activity of free Dox (10 μg/mL) at different pH after 24 h incubation. Clear pH-sensitive and dose-dependent antitumor activity of p(PEGA)$_{30}$-*b*-p(Lys)$_{25}$-*b*-p(His)$_{100}$ vesicles can be observed.

block typically has less effect on the release rate than pH change.

3.6. Cytotoxicity of p(PEGA)$_{30}$-*b*-p(lys)$_{25}$-*b*-p(His)$_n$ Vesicles. The cytotoxicity of the p(PEGA)$_{30}$-*b*-p(Lys)$_{25}$-*b*-p(His)$_n$ was determined using an MTS cell viability assay, with different concentrations of polymers and NIH 3T3 and CT26 cell lines. The cell-only group was used as the positive control (PC), and Triton X100 was used as the negative control (NC). p(PEGA)$_{30}$-*b*-p(Lys)$_{25}$-*b*-p(His)$_n$ polymer-treated cells showed high viability (>94%) over a wide concentration range (0.01−100 μg/mL) (Figure 3). These results revealed no significant difference in the cell viability profiles among the p(PEGA)$_{30}$-*b*-p(Lys)$_{25}$-*b*-p(His)$_n$, irrespective of the chain length of p(His). Generally, p(Lys) is regarded as a toxic polymer, but its toxicity completely depends on the molecular weight (as it results from high cationic charge densities) and the duration of in vivo administration.[46,58] The nontoxicity of the polymers in this study can be attributed to the conjugation of low molecular weight p(Lys) to completely biocompatible polymers (p(PEGA) and p(His)). From the results of in vitro studies, it is evident that the p(PEGA)$_{30}$-*b*-p(Lys)$_{25}$-*b*-p(His)$_n$ polymer has no acute and intrinsic cytotoxicity against normal or cancer cell lines.

3.7. Cellular Uptake of Dox-Loaded p(PEGA)$_{30}$-*b*-p(Lys)$_{25}$-*b*-p(His) Vesicles. To investigate the antitumor effect of Dox-loaded p(PEGA)$_{30}$-*b*-p(Lys)$_{25}$-*b*-p(His)$_n$ vesicles, CT26 cells were treated with Dox-loaded vesicles of p(PEGA)$_{30}$-*b*-p(Lys)$_{25}$-*b*-p(His)$_{100}$ and incubated for 24 h. The Dox-loaded vesicles show clear pH-dependent and dose-dependent (from 0.1 to 10 μg/mL of Dox) cytotoxicity toward CT 26 cells (Figure 4a). The enhanced cellular uptake and toxicity in the endosomal pH range (pH 5−6) demonstrate greater intracellular release of Dox from the vesicles than at pH 7.4. The internalization of free Dox into CT 26 cells at different pH and the resultant cytotoxicity were also compared; the contrary results were observed as expected. We found a very low growth inhibition even with 10 μg of free Dox at different pH conditions studied (Figure 4b). Duong et al. investigated the relative toxicities of free Dox and Dox-loaded nanoparticles in various cell lines.[59] We found that the in vitro half-maximal inhibitory concentration (IC_{50}) values for Dox-loaded p(PEGA)$_{30}$-*b*-p(Lys)$_{25}$-*b*-p(His)$_{100}$ vesicles on CT26 cells are 1.8, 1.3, 1.1, and 0.83 μM at pH 7.4, pH 6.6, pH 6, and pH 5.5, respectively, after 24 h incubation time.

To get an another insight into the pH-sensitive endocytosis and tumor accumulation of the Dox-loaded p(PEGA)$_{30}$-*b*-p(Lys)$_{25}$-*b*-p(His)$_{100}$ vesicles, confocal microscopic observation was carried out. The results clearly demonstrated stronger Dox fluorescence in the cells at acidic pH as compared to pH 7.4 (Figure 5). A major goal in polymeric drug delivery is to design

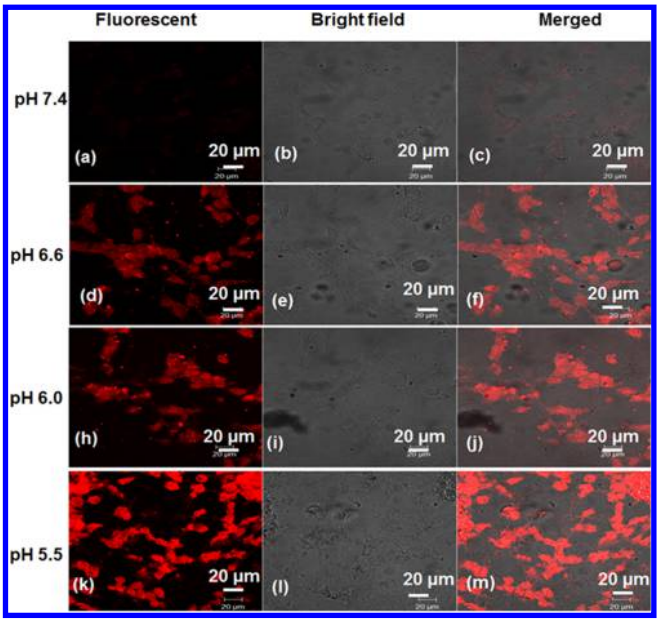

Figure 5. Confocal laser scanning microscopic images of CT26 cells taken after 3 h incubation at pH 7.4 (a−c), at pH 6.6 (d−f), at pH 6 (h−j), and at pH 5.5 (k−m) with Dox-loaded p(PEGA)$_{30}$-*b*-p(Lys)$_{25}$-*b*-p(His)$_{100}$ vesicles (Dox = 10 μg/mL).

a polymer micelles that facilitate an endocytic pathway to deliver a bioactive payload into a malfunctioning cell. However, to examine of the effectiveness of this approach, sufficient information must be collected by combining various techniques, understanding the mechanisms by which cells interact, and internalizing the micelles that are designed to transport therapeutics to target cells. Evidently, it is premature to conclude the effectiveness of pH-sensitive endocytosis only by confocal microscopic observations, because, in these tests, the tumor accumulation is an event outside of the cells and the uptake of released Dox is observed from the vesicles in the medium (outside of the cells).

DOI: 10.1021/acsami.5b05338
ACS Appl. Mater. Interfaces XXXX, XXX, XXX−XXX

Knowledge about the internalization processes of the Dox-loaded $p(PEGA)_{30}$-*b*-$p(Lys)_{25}$-*b*-$p(His)_{100}$ vesicles can be quantitatively analyzed using flow cytometry (FACScan), allowing fast evaluation of a large number of cells, which provides statistically reliable data. CT 26 cells treated with Dox-loaded vesicles were subjected to flow cytometric (FACScan) analysis (Figure S8), demonstrating enhanced fluorescence intensity of Dox-loaded vesicles at endosomal pH rather than at pH 7.4. From these results, we conclude that the vesicles efficiently released Dox via pH-induced destabilization, and this pH-targeted release could be specifically toxic to tumor cells. Similar experiments of free Dox showed low intracellular internalization irrespective of the pH conditions (Figure S9).

4. CONCLUSIONS

Biocompatible and pH-responsive vesicles were successfully fabricated on the basis of $p(PEGA)_{30}$-*b*-$p(Lys)_{25}$-*b*-$p(His)_n$ triblock copolymer synthesized by combining RAFT, ring-opening polymerization of amino acid NCAs, and azide−alkyne click cycloaddition reactions. These stimulus-responsive copolymers were capable of forming hybrid vesicles and effectively internalizing into NIH 3T3 and CT26 cells. The viability of both cell lines is >94% at a wide range of vesicle concentrations (0.1−100 μg/mL). The Dox-encapsulated vesicles preferentially released the drug in acidic environments in CT26 cell lines. These vesicles showed biocompatibility and good loading efficiency of Dox, and they could rapidly cross cell membranes by endocytosis, followed by the endosomal-pH-induced disassembly of the p(His) bilayer, resulting in selective release of Dox into cancer cells. The biocompatible vesicles showing pH-responsiveness hold great promise for efficient intracellular delivery of potent anticancer drugs.

■ ASSOCIATED CONTENT

Supporting Information

The Supporting Information is available free of charge on the ACS Publications website at DOI: 10.1021/acsami.5b05338.

Synthesis and characterization of 1-azido-3-aminopropane, synthesis procedure of α-amino acid *N*-carboxy anhydrides, spectral characterization of RAFT CTA, and its synthetic intermediates, and spectral and GPC characterization of the block copolymers (PDF)

■ AUTHOR INFORMATION

Corresponding Authors

*Tel.: +82-61-379-8481. Fax: 82-61-379-8455. E-mail: pik96@chonnam.ac.kr.

*Tel.: +82-051-510-2466. Fax: +82-051-513-7720. E-mail: ilkim@pusan.ac.kr.

Present Address

[‖]Department of Drug Discovery and Biomedical Sciences, South Carolina College of Pharmacy, University of South Carolina, 715 Sumter Street, Columbia, South Carolina 29208, United States.

Author Contributions

[⊥]R.P.J. and S.U. contributed equally.

Notes

The authors declare no competing financial interest.

■ ACKNOWLEDGMENTS

This work was supported by grants-in-aid for Fusion Research Program for Green Technologies through the National Research Foundation of Korea from MEST (no. 2012M3C1A1054502), BK21 PLUS program, and Bio Imaging Research Center at Gwangju Institute of Science and Technology (GIST), Korea.

■ REFERENCES

(1) Cai, S.; Yang, Q.; Taryn, R.; Bagby, T.; Forrest, M. L. Lymphatic Drug Delivery using Engineered Liposomes and Solid Lipid Nanoparticles. *Adv. Drug Delivery Rev.* **2011**, *63*, 901−908.

(2) Kataoka, K.; Harada, A.; Nagasaki, Y. Block Copolymer Micelles for Drug Delivery: Design, Characterization and Biological Significance. *Adv. Drug Delivery Rev.* **2012**, *64*, 37−48.

(3) Johnson, R. P.; Jeong, Y- I.; Chung, C. W.; Choi, E.; Kang, D. H.; Oh, S. O.; Suh, H.; Kim, I. Biocompatible Poly(2-hydroxyethyl methacrylate)-*b*-poly(L-histidine) Hybrid Materials for pH-sensitive Intracellular Anticancer Drug Delivery. *Adv. Funct. Mater.* **2012**, *22*, 1058−1068.

(4) Johnson, R. P.; Jeong, Y- I.; John, J. V.; Chung, C. W.; Kang, D. H.; Selvaraj, M.; Suh, H.; Kim, I. Dual Stimuli-Responsive poly(*N*-isopropylacrylamide)-*b*-poly(L-histidine) Chimeric Materials for the Controlled Delivery of Doxorubicin into Liver Carcinoma. *Biomacromolecules* **2013**, *14*, 1434−1443.

(5) Meng, F. H.; Zhong, Z. Y.; Feijen, J. Stimuli-Responsive Polymersomes for Programmed Drug Delivery. *Biomacromolecules* **2009**, *10*, 197−209.

(6) Matsumura, Y.; Maeda, H. A New Concept for Macromolecular Therapeutics in Cancer Chemotherapy: Mechanism of Tumoritropic Accumulation of Proteins and the Antitumor Agent Smancs. *Cancer Res.* **1986**, *46*, 6387−6392.

(7) Klibano, A. L.; Maruyama, K.; Torchilin, V. P.; Huang, L. Amphipathic Polyethyleneglycols Effectively Prolong the Circulation Time of Liposomes. *FEBS Lett.* **1990**, *268*, 235−237.

(8) Andresen, T. L.; Jensen, S. S.; Jorgensen, K. Advanced Strategies in Liposomal Cancer Therapy: Problems and Prospects of Active and Tumor Specific Drug Release. *Prog. Lipid Res.* **2005**, *44*, 68−97.

(9) Gabizon, A. A.; Shmeeda, H.; Zalipsky, S. J. Pros and Cons of the Liposome Platform in Cancer Drug Targeting. *J. Liposome Res.* **2006**, *16*, 175−183.

(10) Johnson, R. P.; Jeong, Y- I.; John, J. V.; Chung, C. W.; Choi, S. H.; Song, S. Y.; Kang, D. H.; Suh, H.; Kim, I. Lipo-poly(L-histidine) Hybrid Materials with pH-sensitivity, Intracellular Delivery Efficiency, and Intrinsic Targetability to Cancer Cells. *Macromol. Rapid Commun.* **2014**, *35*, 888−894.

(11) Zhang, L.; Eisenberg, A. Multiple Morphologies of "Crew-cut" Aggregates of Polystyrene-*b*-poly(acrylic acid) Block Copolymers. *Science* **1995**, *268*, 1728−1731.

(12) Discher, D. E.; Eisenberg, A. Polymer vesicles. *Science* **2002**, *297*, 967−973.

(13) Discher, B. M.; Won, Y. Y.; Ege, D. S.; Lee, J. C. M.; Bates, F. S.; Discher, D. E.; Hammer, D. A. Polymersomes: Tough Vesicles Made from Diblock Copolymers. *Science* **1999**, *284*, 1143−1146.

(14) Antonietti, M.; Forster, S. Vesicles and Liposomes: A Self-assembly Principle Beyond Lipids. *Adv. Mater.* **2003**, *15*, 1323−1333.

(15) Yu, K.; Eisenberg, A. Bilayer Morphologies of Self-assembled Crew-cut Aggregates of Amphiphilic PS-*b*-PEO Diblock Copolymers in Solution. *Macromolecules* **1998**, *31*, 3509−3518.

(16) Shen, H.; Eisenberg, A. Control of Architecture in Block-Copolymer Vesicles. *Angew. Chem., Int. Ed.* **2000**, *39*, 3310−3312.

(17) Kukula, H.; Schlaad, H.; Antonietti, M.; Forster, S. The Formation of Polymer Vesicles or "Peptosomes" by Polybutadiene-*block*-poly(L-glutamate)s in Dilute Aqueous Solution. *J. Am. Chem. Soc.* **2002**, *124*, 1658−1663.

(18) Checot, F.; Brulet, A.; Oberdisse, J.; Gnanou, Y.; Mondain-Monval, O.; Lecommandoux, S. Structure of Polypeptide-based

DOI: 10.1021/acsami.5b05338
ACS Appl. Mater. Interfaces XXXX, XXX, XXX−XXX

Diblock Copolymers in Solution: Stimuli-Responsive Vesicles and Micelles. *Langmuir* **2005**, *21*, 4308−4315.
(19) Geng, Y.; Ahmed, F.; Bhasin, N.; Discher, D. E. Visualizing Worm Micelle Dynamics and Phase Transitions of a Charged Diblock Copolymer in Water. *J. Phys. Chem. B* **2005**, *109*, 3772−79.
(20) Checot, F.; Rodrıguez-Hernandez, J.; Gnanou, Y.; Lecommandoux, S. pH-responsive Micelles and Vesicles Nanocapsules Based on Polypeptide Diblock Copolymers. *Biomol. Eng.* **2007**, *24*, 81−85.
(21) Sigel, R.; Losik, M.; Schlaad, H. pH Responsiveness of Block Copolymer Vesicles with a Polypeptide Corona. *Langmuir* **2007**, *23*, 7196−7199.
(22) Gebhardt, K. E.; Ahn, S.; Venkatachalam, G.; Savin, D. A. Role of Secondary Structure Changes on the Morphology of Polypeptide-based Block Copolymer Vesicles. *J. Colloid Interface Sci.* **2008**, *317*, 70−76.
(23) Holowka, E. P.; Pochan, D. J.; Deming, T. J. Charged Polypeptide Vesicles with Controllable Diameter. *J. Am. Chem. Soc.* **2005**, *127*, 12423−12428.
(24) Matyjaszewski, K.; Xia, J. Atom Transfer Radical Polymerization. *Chem. Rev.* **2001**, *101*, 2921−2990.
(25) Boyer, C.; Bulmus, V.; Davis, T. P.; Ladmiral, V.; Liu, J.; Perrier, S. Bioapplications of RAFT Polymerization. *Chem. Rev.* **2009**, *109*, 5402−5436.
(26) Hadjichristidis, N.; Iatrou, H.; Pitsikalis, M.; Sakellariou, G. Synthesis of Well-Defined Polypeptide-based Materials via the Ring-opening Polymerization of α-amino acid *N*-Carboxyanhydrides. *Chem. Rev.* **2009**, *109*, 5528−78.
(27) Rostovtsev, V. V.; Green, L. G.; Fokin, V. V.; Sharpless, K. B. A Stepwise Huisgen Cycloaddition Process: Copper(I)-Catalyzed Regioselective "Ligation" of Azides and Terminal Alkynes. *Angew. Chem., Int. Ed.* **2002**, *41*, 2596−99.
(28) Kolb, H. C.; Finn, M. G.; Sharpless, K. B. Click Chemistry: Diverse Chemical Function from a Few Good Reactions. *Angew. Chem., Int. Ed.* **2001**, *40*, 2004−2021.
(29) Rodrıguez-Hernandez, J.; Lecommandoux, S. Reversible Inside−Out Micellization of pH-Responsive and Water-Soluble Vesicles Based on Polypeptide Diblock Copolymers. *J. Am. Chem. Soc.* **2005**, *127*, 2026−2027.
(30) Huang, J.; Bonduelle, C.; Thevenot, J.; Lecommandoux, S.; Heise, A. Biologically Active Polymersomes from Amphiphilic Glycopeptides. *J. Am. Chem. Soc.* **2012**, *134*, 119−122.
(31) Upadhyay, K. K.; Le Meins, J- F.; Misra, A.; Voisin, P.; Bouchaud, V.; Ibarboure, E.; Schatz, C.; Lecommandoux, S. Biomimetic Doxorubicin Loaded Polymersomes from Hyaluronan-*block*-poly(γ-benzyl glutamate) Copolymers. *Biomacromolecules* **2009**, *10*, 2802−2808.
(32) Upadhyay, K. K.; Bhatt, A. N.; Mishra, A. K.; Dwarakanath, B. S.; Schatz, C.; Le Meins, J−F.; Farooque, A.; Chandraiah, G.; Jain, A. K.; Misra, A.; Lecommandoux, S. The Intracellular Drug Delivery and Anti-Tumor Activity of Doxorubicin Loaded Poly(gamma-benzyl L-glutamate)-*b*-hyaluronan Polymersomes. *Biomaterials* **2010**, *31*, 2882−2892.
(33) Schatz, C.; Louguet, S.; Le Meins, J- F.; Lecommandoux, S. Polysaccharide-block-Polypeptide Copolymer Vesicles: Towards Synthetic Viral Capsids. *Angew. Chem., Int. Ed.* **2009**, *48*, 2572−75.
(34) Sanson, C.; Schatz, C.; Le Meins, J.-F.; Brulet, A.; Soum, A.; Lecommandoux, S. Biocompatible and Biodegradable poly(trimethylene carbonate)-*b*-poly(L-glutamic acid) Polymersomes: Size Control and Stability. *Langmuir* **2010**, *26*, 2751−2760.
(35) Sanson, C.; Schatz, C.; Le Meins, J.-F.; Soum, A.; Thevenot, J.; Garanger, E.; Lecommandoux, S. A Simple Method to Achieve High Doxorubicin loading in Biodegradable Polymersomes. *J. Controlled Release* **2010**, *147*, 428−435.
(36) Sanson, C.; Diou, O.; Thevenot, J.; Ibarboure, E.; Soum, A.; Brulet, A.; Miraux, S.; Thiaudiere, E.; Tan, S.; Brisson, A.; Dupuis, V.; Sandre, O.; Lecommandoux, S. Doxorubicin Loaded Magnetic Polymersomes: Theranostic Nanocarriers for MR Imaging and Magneto-Chemotherapy. *ACS Nano* **2011**, *5*, 1122−1140.
(37) Marguet, M.; Edembe, L.; Lecommandoux, S. Polymersomes in Polymersomes: Multiple Loading and Permeability Control. *Angew. Chem., Int. Ed.* **2012**, *51*, 1173−1176.
(38) Agut, W.; Brulet, A.; Schatz, C.; Taton, D.; Lecommandoux, S. pH and Temperature Responsive Polymeric Micelles and Polymersomes by Self-assembly of poly[2-(dimethylamino)ethyl methacrylate]-*b*-poly(glutamic acid) Double Hydrophilic Block Copolymers. *Langmuir* **2010**, *26*, 10546−10554.
(39) Lee, E. S.; Gao, Z.; Bae, Y. H. Recent Progress in Tumor pH Targeting Nanotechnology. *J. Controlled Release* **2008**, *132*, 164−170.
(40) Priya, B.; Viness, P.; Yahya, E. C.; Lisa, C. d. T. Stimuli-Responsive Polymers and their Applications in Drug Delivery. *Biomed. Mater.* **2009**, *4*, 022001.
(41) Napoli, A.; Boerakker, M. J.; Tirelli, N.; Nolte, R. J. M.; Sommerdijk, N. A. J. M.; Hubbell, J. A. Glucose-oxidase Based Self-destructing Polymeric Vesicles. *Langmuir* **2004**, *20*, 3487−3491.
(42) Meng, F.; Hiemstra, C.; Engbers, G. H. M.; Feijen, J. Biodegradable Polymersomes. *Macromolecules* **2003**, *36*, 3004−3006.
(43) Yin, H.; Kang, S.-W.; Bae, Y. H. Polymersome Formation from AB_2 type 3-miktoarm Star Copolymers. *Macromolecules* **2009**, *42*, 7456−7464.
(44) Chen, W.; Meng, F.; Cheng, R.; Zhong, Z. pH-sensitive Degradable Polymersomes for Triggered Release of Dnticancer Drugs: A Comparative Study with Micelles. *J. Controlled Release* **2010**, *142*, 40−46.
(45) Du, Y.; Chen, W.; Zheng, M.; Meng, F.; Zhong, Z. pH-sensitive Degradable Chimaeric Polymersomes for the Intracellular Release of Doxorubicin Hydrochloride. *Biomaterials* **2012**, *33*, 7291−99.
(46) Koide, A.; Kishimura, A.; Osada, K.; Jang, W- D.; Yamasaki, Y.; Kataoka, K. Semipermeable Polymer Vesicle (PICsome) Self-assembled in Aqueous Medium from a pair of Oppositely Charged Block Copolymers: Physiologically Stable Micro-/nanocontainers of Water-soluble Macromolecules. *J. Am. Chem. Soc.* **2006**, *128*, 5988−5989.
(47) Iatrou, H.; Dimas, K.; Gkikas, M.; Tsimblouli, C.; Sofianopoulou, S. Polymersomes from Polypeptide Containing Triblock co- and Terpolymers for Drug Delivery Against Pancreatic Cancer: Asymmetry of the External Hydrophilic Blocks. *Macromol. Biosci.* **2014**, *14*, 1222−38.
(48) Ray, J. G.; Naik, S. S.; Hoff, E. A.; Johnson, A. J.; Ly, J. T.; Easterling, C. P.; Patton, D. L.; Savin, D. A. Stimuli-responsive Peptide-based ABA-triblock Copolymers: Unique Morphology Transitions with pH. *Macromol. Rapid Commun.* **2012**, *33*, 819−826.
(49) Yin, H.; Kang, H. C.; Huh, K. M.; Bae, Y. H. Biocompatible, pH-sensitive AB_2 Miktoarm Polymer-based Polymersomes: Preparation, Characterization, and Acidic pH-activated Nanostructural Transformation. *J. Mater. Chem.* **2012**, *22*, 19168−19178.
(50) Quadir, M. A.; Morton, S. W.; Deng, Z. J.; Shopsowitz, K. E.; Murphy, R. P.; Epps, T. H., III; Hammond, P. T. PEG−polypeptide Block Copolymers as pH-responsive Endosome-Solubilizing Drug Nanocarriers. *Mol. Pharmaceutics* **2014**, *11*, 2420−2430.
(51) Boyer, C.; Liu, J.; Bulmus, V.; Davis, T. P.; Barner-Kowollik, C.; Stenzel, M. H. Direct Synthesis of Well-defined Heterotelechelic Polymers for Bioconjugations. *Macromolecules* **2008**, *41*, 5641−5650.
(52) Bays, E.; Tao, L.; Chang, C.-W.; Maynard, H. D. Synthesis of Semitelechelic Maleimide poly(PEGA) for Protein Conjugation by RAFT Polymerization. *Biomacromolecules* **2009**, *10*, 1777−1781.
(53) Uster, P. S.; Deamer, D. W. pH-Dependent Fusion of Liposomes using Titratable Polycations. *Biochemistry* **1985**, *24*, 1−8.
(54) Benns, J. M.; Choi, J. S.; Mahato, R. I.; Park, J. S.; Kim, S. W. pH-sensitive Cationic Polymer Gene Delivery Vehicle: *N*-Ac-poly(L-histidine)-graft-poly(L-lysine) Comb Shaped Polymer. *Bioconjugate Chem.* **2000**, *11*, 637−645.
(55) Bates, F. S.; Fredrickson, G. H. Block Copolymer Thermodynamics: Theory and Experiment. *Annu. Rev. Phys. Chem.* **1990**, *41*, 525−57.
(56) Rodriguez, A. R.; Choe, U.-J.; Kamei, D. T.; Deming, T. J. Fine Tuning of Vesicle Assembly and Properties Using Dual Hydrophilic Triblock Copolypeptides. *Macromol. Biosci.* **2012**, *12*, 805−811.

DOI: 10.1021/acsami.5b05338
ACS Appl. Mater. Interfaces XXXX, XXX, XXX−XXX

(57) Lee, Y. J.; Kang, H. C.; Hu, J.; Nichols, J. W.; Jeon, Y. S.; Bae, Y. H. pH-Sensitive Polymeric Micelle-Based pH Probe for Detecting and Imaging Acidic Biological Environments. *Biomacromolecules* **2012**, *13*, 2945−2951.
(58) Titlow, W. B.; Lee, C. H.; Ryou, C. Characterization of Toxicological Properties of L-Lysine Polymers in CD-1 mice. *J. Microbiol. Biotechnol.* **2013**, *23*, 1015−1022.
(59) Duong, H. T. T.; Hughes, F.; Sagnella, S.; Kavallaris, M.; Macmillan, A.; Whan, R.; Hook, J.; Davis, T. P.; Boyer, C. Functionalizing Biodegradable Dextran Scaffolds Using Living Radical Polymerization: New Versatile Nanoparticles for the Delivery of Therapeutic Molecules. *Mol. Pharmaceutics* **2012**, *9*, 3046−3061.

DOI: 10.1021/acsami.5b05338
ACS Appl. Mater. Interfaces XXXX, XXX, XXX−XXX